Engineering Science and Technology, an International Journal 20 (2017) 1155–1165

HOSTED BY

Contents lists available at ScienceDirect

Engineering Science and Technology, an International Journal

journal homepage: www.elsevier.com/locate/jestch

Full Length Article

Acetylation, crystalline and morphological properties of structural polysaccharide from shrimp exoskeleton

O.P. Gbenebor [a,*], S.O. Adeosun [a], G.I. Lawal [a], S. Jun [b], S.A. Olaleye [c]

[a] Department of Metallurgical and Materials Engineering, University of Lagos, Nigeria
[b] School of Materials Science, Soochow University, Suzhou, China
[c] Department of Mechanical Engineering, University of Lagos, Nigeria

ARTICLE INFO

Article history:
Received 7 December 2016
Revised 21 March 2017
Accepted 16 May 2017
Available online 25 May 2017

Keywords:
α-Chitin
Acetylation
Crystalline index
Hydrogen bond
SEM/EDS

ABSTRACT

The extraction of a structural polysaccharide, α-chitin, from shrimp exoskeleton via chemical means using hydrochloric acid (HCl) and sodium hydroxide (NaOH) has been done. Concentrations of 0.4, 0.8 and 1.2 M for both HCl and NaOH were chosen to evaluate the acetylation degree (DA), crystalline structure and morphology of the chitin. The *N*-acetyl groups' content in the structural polysaccharide ranged between 65.6 and 99.4% in decreasing order of both acid and alkali concentrations combination used. The magnitude of chitin average hydrogen bond energy E_H was majorly influenced by OH(6)...OC intra and CO...HN intermolecular hydrogen bonds as they showed more predominance than OH(3)...O(5) and OH...OC intra and intermolecular hydrogen bonds. Chitin diffraction planes, crystalline index (CrI) and crystallite size (D_{hkl}) were investigated by X-ray diffraction (XRD) with reflections observed on (021), (110), (130) and (013) planes. The CrI occurred between 79.4 and 87.4%, while crystallite sizes were between 0.544 and 3.64 Å for the samples. Morphological study using scanning electron microscopy with energy dispersive spectroscopy SEM/EDS showed strong calcium and oxygen peaks. This established the shrimp shell surface to be composed of calcite and trace elements such as nitrogen and silicon. The observed α-chitin rough surfaces were attributed to the low degree deacetylation recorded during alkali treatment.

1. Introduction

Chitin is a linear polymer of amino sugars – β-(1→4) – linked 2-acetamido-2-deoxy-β-D-glucopyranose (GlcNAc) and or β-(1→4)-linked 2-amino-2-deoxy-β-D-glucopyranose (GlcN) units [31]. It is known to be a copolymer of *N*-acetyl-D-glucosamine and D-glucosamine units linked with β-(1–4) glycosidic bond, having predominantly *N*-acetyl-D-glucosamine units in the polymeric chain [15]. Chitin ranks second in abundance to cellulose as natural polymers and serves as structural components supporting cell and body surfaces [16]. Its biological functions and chemical structure are similar to cellulose as a structural polysaccharide. However, it differs from cellulose as it contains an acetamide group instead of hydroxyl group at the C-2 position within the glucose unit and it is therefore regarded as a cellulose derivative with an acetamido group [27]. The chitin enhances the mechanical strength of fungal cell walls and exoskeletons of arthropods [20,18].

Crustacean shells are natural sources of chitin as they consist of (20–30%) chitin, (30–40%) proteins, (30–50%) calcium carbonate and the rest pigments (astaxanthin, canthaxanthin, lutein or β-carotene). The proportions of these constituents are dependent on the species and season in which the marine animal exists [5]. In skeletal tissue, chitin combines with protein to form protein-chitin matrix calcified to produce hard shells [30]. The shells may also contain lipids from the muscle residues and carotenoids of astaxanthin and its esters [3]. These constituents must be quantitatively removed to produce high purity biopolymer needed for biological applications. Two ways of doing this is either chemically or biologically. Biological extraction studies have reported that the use of proteolytic enzymes for protein digestion or using microorganism that allows digestion of both proteins and minerals in a fermentation process is a common method used [6]. Chemical treatment on the other hand, is a procedure [2] that entails the use of acid and alkali solutions for the removal of mineral and proteins respectively. The degree of acetylation (DA) is used to identify chitin or its derivative and it is the number of acetyl groups in the

* Corresponding author.
E-mail addresses: ogbenebor@unilag.edu.ng, gbenebor.unilag@gmail.com (O.P. Gbenebor).

Peer review under responsibility of Karabuk University.

http://dx.doi.org/10.1016/j.jestch.2017.05.002
2215-0986/

polysaccharide. In another way, it is the ratio of *N*-acetylated group to *N*-de acetylated (amino) groups [21]. For DA >50%, chitin is formed [15] otherwise its derivative, chitosan is formed. Physical, chemical and biological properties of chitin are strongly dependent on its DA value. Therefore, DA is an important parameter that influences the performance of chitin in applications such as food component and medical fields [17,22]. Several studies have shown that chitin quality is dependent on its source, DA, treatment duration, temperature and type of reagent used [14,28]. In this present study, α-chitin is extracted from exoskeleton of shrimps via chemical treatment with the use of acid and alkali solutions at varying concentrations. Considering a constant treatment temperature and duration, the influence of this treatment on the crystallinity, DA and morphology of α-chitin are investigated.

2. Materials and methods

2.1. Chitin extraction

Shells of shrimp were scraped free of loose tissues, washed, dried and ground with the use of a steel ball mil. The ground particles were sieved to size $250\mu m$ using a standardized sieve of 60BSS. Demineralization was carried out at room temperature (32 °C) by soaking 100 g of ground samples in 0.4, 0.8 and 1.2 M HCl. For each concentration, the process was repeated several times until evolution of gas ceased. The demineralized samples were washed with distilled water to neutral (pH 7.0), filtered and dried in the oven at 70 °C for 4 h to constant weights. Deproteinization was carried out on each sample by heating mineral - devoid samples in concentrations of 0.4, 0.8 and 1.2 M NaOH solutions in a beaker at 100 °C for 1 h. At the end of this period, samples were filtered and soaked in fresh sets of alkali solutions (0.4, 0.8 and 1.2 M) for 18 h at 32 °C for effective protein removal. The samples were washed with distilled water to pH 7.0, filtered and oven dried at 70 °C. Depigmentization was carried out by soaking extracted chitin in 1 M H_2O_2 for 24 h at 32 °C. The chitin was washed in distilled water and dried for 4 h in an oven (70 °C) before characterizations.

2.2. Characterizations of extracted chitin

2.2.1. Acetylation degree measurement (DA) using Fourier Transform Infrared spectroscopy (FTIR)

A Nicolet 6700 M spectrometer in transmission mode was used in carrying out FTIR spectra of samples. Ten milligram of fine samples were dispersed in a matrix of KBr (500 mg), followed by compression at 22–30 MPa to form pellets. The transmittance measurements were carried out in the range of 400–4000 cm^{-1} at a resolution of 4 cm^{-1}. This was carried out in Redeemers University, Nigeria. The DA was calculated using Eq. (1) [14]:

$$DA = [(A1650/A3450) \times 100/1.33] \quad (1)$$

where: A_{1650} is the absorbance of amide I vibration; A_{3450}, absorbance of OH vibration; 1.33 is a factor that represents the ratio of A_{1650}/A_{3450} for fully N-acetylated chitin.

2.2.2. X-Ray diffraction (XRD)

The XRD of each sample was conducted using PANanalytical X' Pert PRO MPD X-ray diffraction system PW3040/60 machine at Soochow University, China. Samples were exposed to a monochromatic Cu Kα radiation (k = 1.5406 Å), operating at 40 kV and 40 mA. Crystallinity index (CrI) determination for chitin was done using Eq. (2) [13].

$$CrI(\%) = [I_c/(I_c + I_a)] \times 100 \quad (2)$$

where I_c and I_a represent the intensities of the crystalline and amorphous regions respectively. Crystalline size normal to the h k l plane (D_{hkl}) was calculated from the full width of peak at half height of the source curve using Eq. (3) [2,28].

$$Dhkl = k\lambda/\beta\cos\theta \quad (3)$$

Where K is a constant (indicative of crystallite perfection and is assumed to be 1); λ(Å)is the wave length of incident radiation (1.5406 Å); β (rad) is the width of the crystalline peak at half height and θ (deg) is the diffraction angle corresponding to the crystalline peak.

2.2.3. Scanning electron microscopy (SEM) with energy dispersive X-ray Analysis (EDS)

An ASPEX 3020 model variable pressure SEM operated with an electron intensity beam 15 kV and equipped with Noran-Voyager energy dispersive spectroscope (situated in Covenant University, Nigeria) was used to observe the morphological features of all samples. The samples to be observed under the SEM were mounted on a conductive carbon imprint left by the adhesive tape prepared by placing the samples on the circular holder and coated for 5 min to enable it conduct electricity. For EDS analysis, samples were analyzed at an accelerating voltage of 15 kV.

2.2.4. Thermogravimetric Analysis (TGA)

Analysis of samples was carried out on TGA Q500 instrument where 2 mg of samples were heated to 750 °C at 10 °C/minute heating rate. In this test, the temperature for the onset of thermal decomposition (T_{onset}), temperature at the end of decomposition (T_{finish}), the temperature at which decomposition rate was rapid (T_{max}) and chitin content were deduced from the thermograms.

3. Results and discussion

3.1. Acetylation degree (DA)

Fig. 1 shows the DA of extracted chitin with concentrations of HCl and NaOH solutions. The DA has a maximum value of 99.4% when ground shrimp shells are treated with 0.4 M HCl and 0.4 M NaOH. This implies that the number of glucopyranose units with *N*-acetyl groups in this biopolymer is the highest compared to chitin obtained using 0.8 and 1.2 M NaOH at 0.4 M HCl (79.5 and 74.3%). The minimum DA (65.6%) is recorded for shrimp chitin obtained at 1.2 M HCl and 1.2 M NaOH. Here, the resistance of acetamide groups imposed by the *trans* arrangement of the C2-C3 substituents in the sugar ring is lowered by high concentrations of reagents. Thus, this study has shown that HCl and NaOH can induce partial removal of the *N*-acetyl groups resulting in DA decrease as concentration increases.

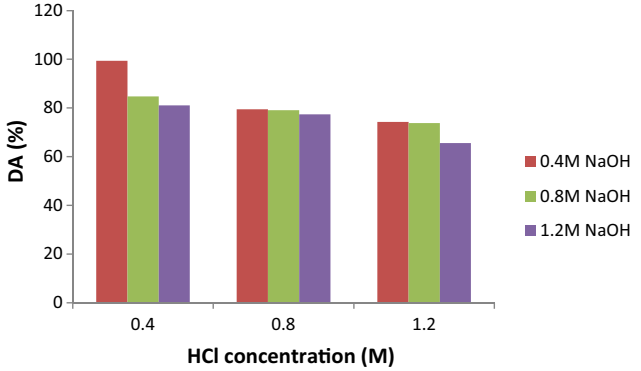

Fig. 1. DA of extracted chitin with HCl and NaOH concentrations.

3.2. FTIR

The FTIR spectrum of virgin shrimp shell (Fig. 2) shows that there are different functional groups detected on its surface. Broad peaks detected between 3500 and 3200 cm^{-1} could be assigned to O—H stretching of the water molecule and N—H groups. The peak at 2852 cm^{-1} corresponds to C–H stretching vibrations of aliphatic hydrocarbons (alkane groups) while the peak at 1653 cm^{-1} is caused by stretching vibrations of C=O (amide I). A small absorption band occurring at 2521 cm^{-1} represents carboxylic acid (—COOH). Absorption peaks at 1796, 14,566 and 874 cm^{-1} represent stretching and bending vibrations of calcite, $CaCO_3$ [23]. .Absorption band at 1423 cm^{-1} confirms the presence of CH_3 bending and CH_2 deformation.

Analysis of the chitin FTIR spectra extracted chemically from shrimp shell (Fig. 3) at varying concentrations of acid and alkali show the presence of O—H and NH groups occurring in the range 3496–3372 cm^{-1} and 3265–3100 cm^{-1} respectively. Spectrum at 2933 cm^{-1} represents stretching vibrations of C—H (CH_3 and CH_2). The most important signals in the spectrum of chitin are the peaks at 1661, 1559 and 1312 cm^{-1} with characteristic stretching vibrations of amides I, II and III bands. Two amide I peaks are observed at 1661 and 1626 cm^{-1} showing that the chitin structure obtained from the shrimp shell is the α-form. The spectrum also features peaks at 1157, 1074 and 1028 cm^{-1} relating to the presence of C—O—C bonds in the structure. At varying reagent concentrations, chitin has shown to possess similar spectra as no new band is formed and functional groups exist on the same wavenumber except in the OH-NH broad band region where there are few shifts (Fig. 3). It is also observed that at a particular NaOH concentration, intensity of bands decrease with increasing HCl concentrations. In addition, the area within the broad OH-NH band at 3600–3000 cm^{-1} decreases when the concentration of HCl is increased for a particular NaOH concentration. The table showing a summary of vibration modes of virgin shrimp shell and α–chitin extracted from shrimp shell is shown in Table 1.

Conformational and mechanical properties of structural polysaccharides have been affirmed to be influenced by two intra molecular and intermolecular hydrogen bonds [8]. The first intra molecular hydrogen bond occurs when a carbonyl group on C-2 bonds to the hydroxyl group on C-6 i.e. O H(6)···O=C (Fig. 4a) while the second exists between the OH group on C-3 and the ring oxygen (OH (3)···O-5) [32]. The bands related to NH of the amide group lie between 3265 and 3010 cm^{-1}. They are assigned to the vibration modes involved in strong intermolecular hydrogen bond

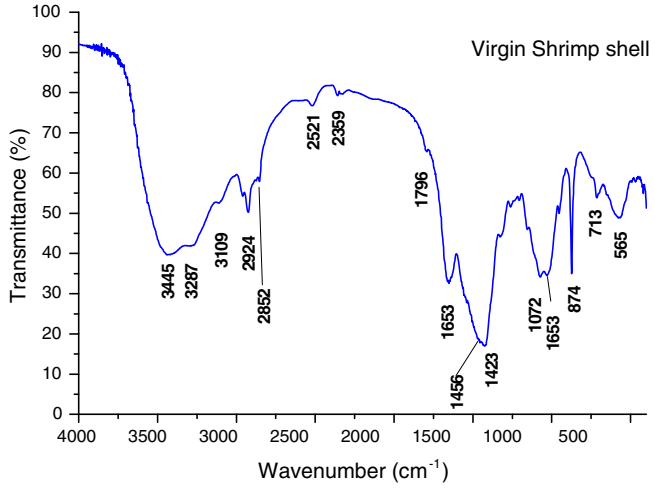

Fig. 2. FTIR spectra of virgin shrimp shell.

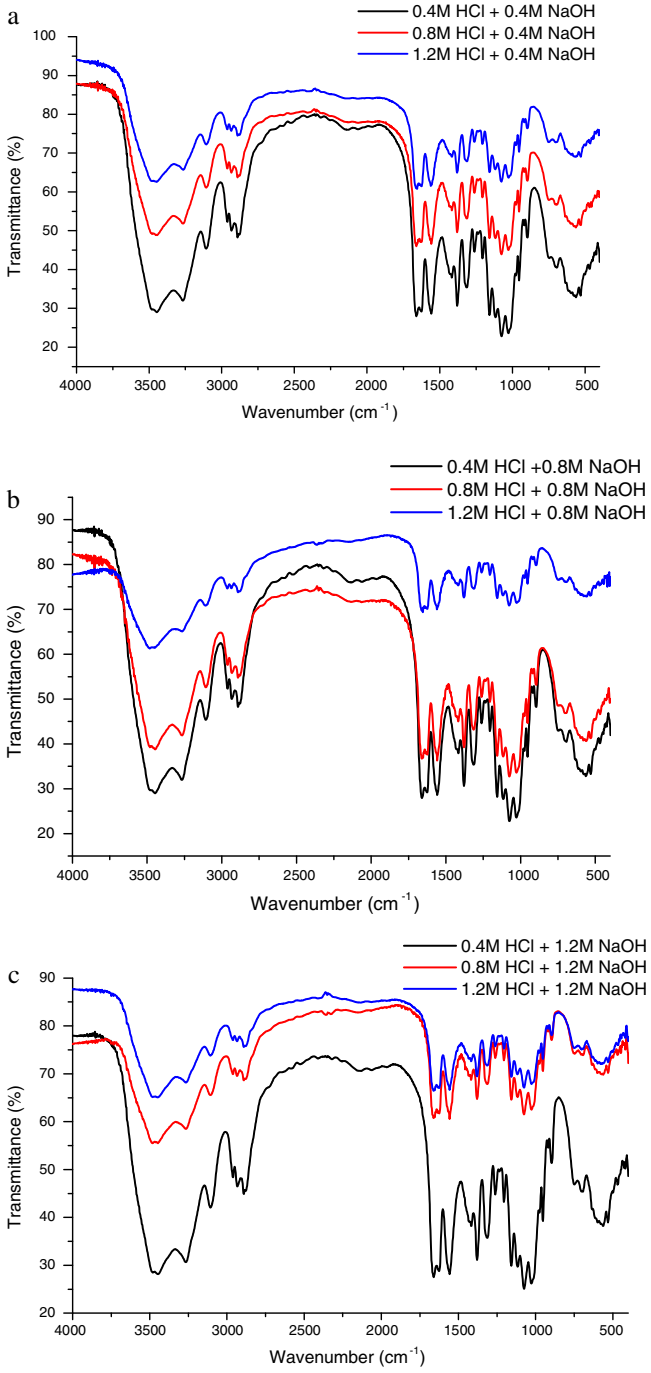

Fig. 3. FTIR spectra of shrimp chitin extracted with different acid concentrations and (a) 0.4 M (b) 0.8 M (c) 1.2 M alkali.

networks of C=O···HN and OH···O=C respectively as shown in Fig. 4b [25,33]).

Chitin with high hydrogen bond occupancy is concluded to possess a greater resistance to fracture [9]. To study this in shrimp chitin, broad and overlapped FTIR absorption spectra existing between 3600 and 3000 cm^{-1} were resolved and improved by their deconvolution from a background scattering using a Gaussian function curve-fitting analysis with an $r^2 > 0.99$. Spectrum fitting of a sample is shown in Fig. 5.

The energy of the hydrogen bond, E_H (kCal) was calculated using Eq. (4) [8]:

$$E_H = [1/k \times (V_o - V)/V_o] \quad (4)$$

Table 1
Vibration modes of samples from FTIR.

Vibration modes	Wavenumber (/cm)	
	Shrimp shell	shrimp chitin
OH stretching	3444	3496–3460
NH stretching	3390	3265
NH stretching	3109	3100
Symmetric Ch3 stretching and assymetric CH2 stretching	2924	2934
CH stretching	2852	2878
C=O secondary amide stretch (amide I)	1653	1661
C=O secondary amide stretch (amide I)	–	1626
NH bend, CN stretch (amide II)	–	1559
CH2 bending and CH3 deformation	1423	1416
CH bending and Ch3 symmetric deformation	–	1379
CH2 wagging (amide III)	–	1312
Asymmetric bridge oxygen stretching	–	1157
Asymmetric in-phase ring stretching mode	–	1117
C—O—C assymetric stretch in phase ring	1072	1074
CO stretching	–	1028
CH3 wagging along chain	953	953
CH stretching (saccharide rings)	–	897
NH out-plane bending	713	750
OH out-of-plane bending	–	694
Calcium carbonate	1796. 1456, 874	–

where: V_o is the standard frequency corresponding to free OH groups (3600 cm^{-1}); V is the frequency of the bonded OH groups and k = 1.68 × 10^{-2} $kcal^{-1}$.

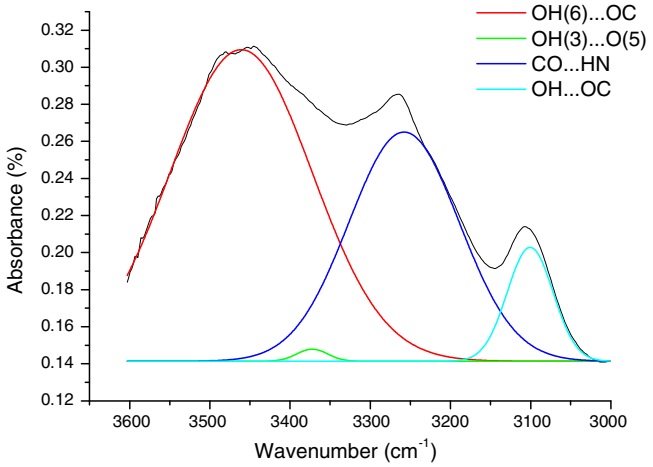

Fig. 5. Spectrum fitting of hydrogen region for shrimp chitin.

The OH(6)...OC and OH(3)...O(5) intra molecular hydrogen bonds are formed between 3464–3458 cm^{-1} and 3374–3464 cm^{-1} respectively (Table 2) while CO...HN and OH...OC intermolecular hydrogen bonds are formed between 3249–3264 cm^{-1} and 3100–3102 cm^{-1}. The E_H for OH(6)...OC, OH(3)...O(5), CO...HN and OH...OC measure 3.31, 3.77, 5.65 and 8.27 kCal respectively for chitin extracted from 0.4 M HCl and 0.4 M NaOH. Increasing the acid concentration to 0.8 and 1.2 M lowers the values from 5.22 (at 0.4 M HCl) to 4.98 and 4.64kCal, which confirms gradual cleavage of hydrogen bonds. Shrimp chitin extracted using

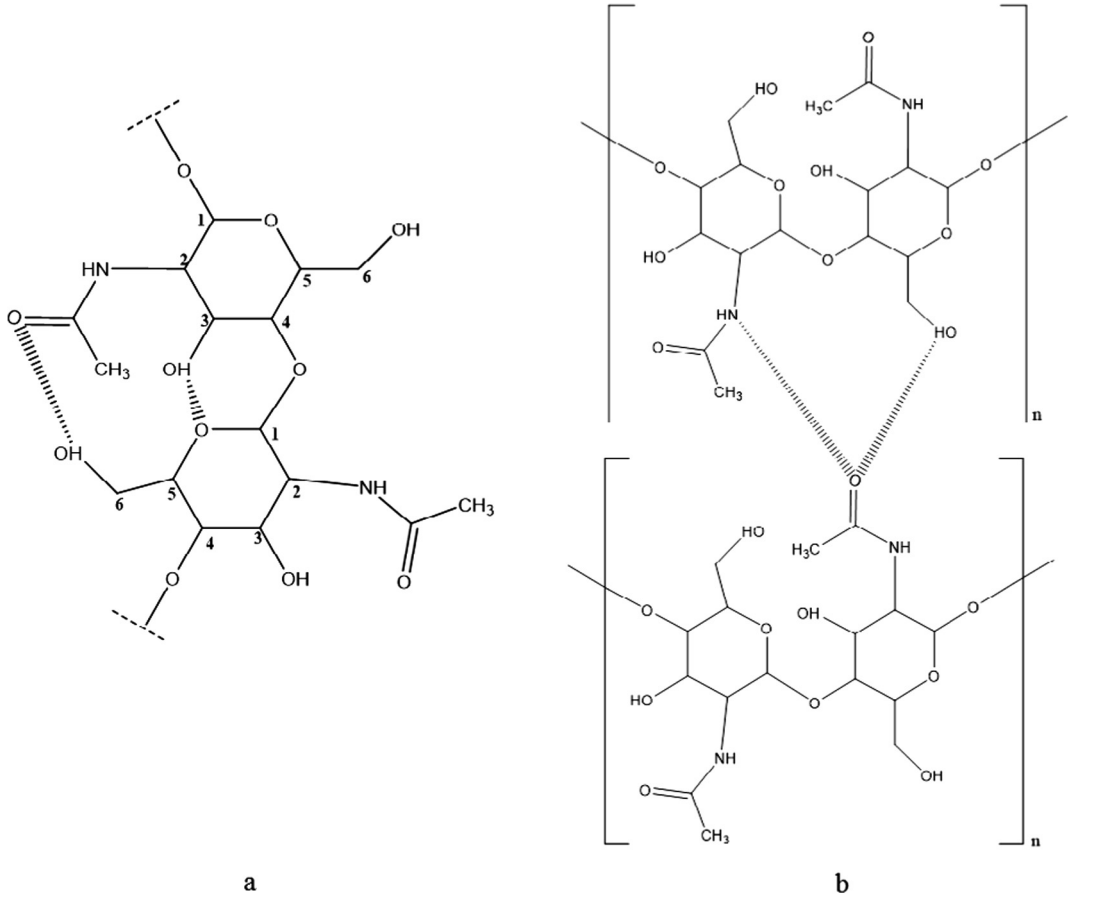

Fig. 4. (a) Intra and (b) intermolecular hydrogen pattern in chitin monomer.

Table 2
FTIR absorption band assignment to the OH band (3600–3000 cm^{-1}) for shrimp chitin.

samples	OH(6)...OC			OH(3)—O(5)			CO...HN			OH...OC			
Reagent ratio (acid:alkali)	cm^{-1}	Amount (%)	E_H (kCal)	cm^{-1}	Amount (%)	E_H (kCal)	cm^{-1}	Amount (%)	E_H (kCal)	cm^{-1}	Amount (%)	E_H (kCal)	Average E_H (kCal)
0.4;0.4	3460	58.9	3.31	3372	2.32	3.77	3258	33.63	5.65	3100	5.15	8.27	5.25
0.4;0.8	3460	55.65	3.31	3371	1.93	3.79	3264	35.5	5.56	3102	6.92	8.23	5.22
0.4;1.2	3461	59.94	2.3	3374	2.28	3.74	3265	30.97	5.61	3102	6.81	8.23	4.99
0.8;0.4	3464	57.66	2.25	3374	1.76	3.74	3258	33.59	5.65	3100	6.99	8.27	4.98
0.8;0.8	3462	54.6	2.28	3372	2	3.77	3264	38	5.56	3100	5.4	8.27	4.97
0.8;1.2	3458	51.87	2.35	3458	7.76	2.35	3261	37.39	5.61	3101	2.98	8.25	4.64
1.2;0.4	3464	53.1	2.25	3464	22.3	2.25	3249	19.5	5.8	3100	5.1	8.27	4.64
1.2;0.8	3459	28.43	2.33	3459	28.5	2.33	3260	35.23	5.62	3101	7.84	8.25	4.63
1.2;1.2	3463	49.8	2.25	3464	19.7	2.25	3249	24.2	5.8	3100	6.3	8.27	4.62

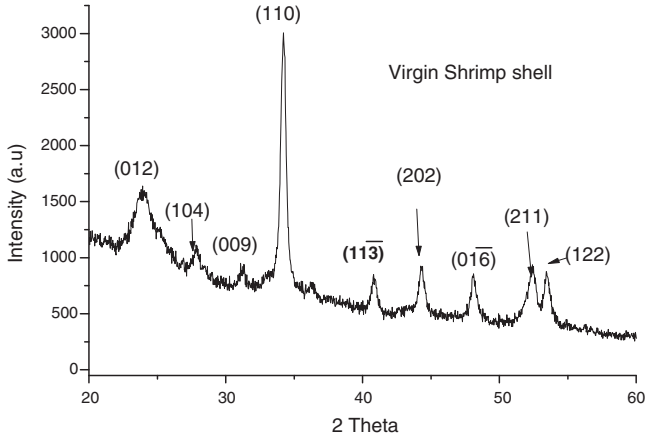

Fig. 6. XRD of virgin shrimp shell.

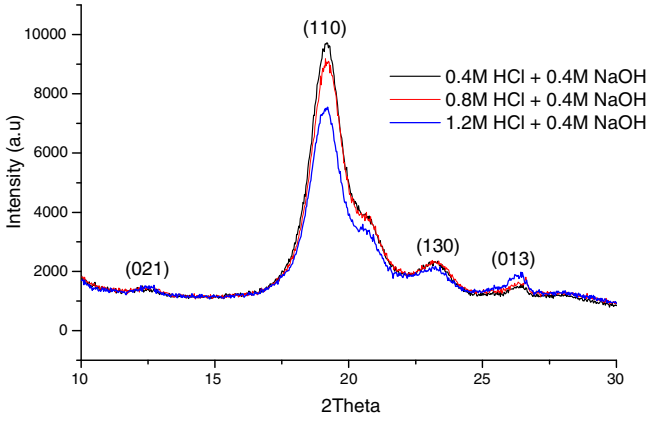

Fig. 7. XRD of shrimp chitin extracted with HCl concentrations at 0.4 M NaOH.

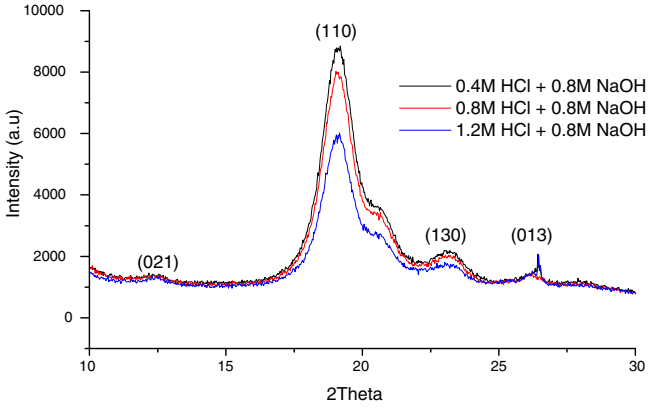

Fig. 8. XRD of shrimp chitin extracted with HCl concentrations at 0.8 M NaOH.

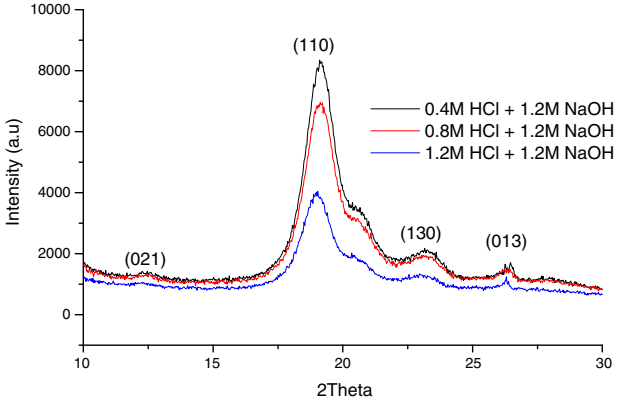

Fig. 9. XRD of shrimp chitin extracted with HCl concentrations at 1.2 M NaOH.

0.4 M HCl and 0.8 M NaOH has its OH(6)...OC, OH(3)...O(5), CO...HN and OH...OC intra and intermolecular hydrogen bonds existing at 3460, 3371, 3264 and 3102 cm^{-1} respectively. The intra molecular OH(6)...OC bond occupies the largest portion (55.65%) of the hydrogen bonds within this broad band followed by 33.50%, occupied by CO...HN, 6.92% by OH...OC and OH(3)...O (5) occupying the least (1.93%). The average E_H is high for this sample and calculated as 5.22 kCal. With the same alkali concentration (0.8 M), OH(6)...OC, OH(3)...O(5), CO...HN and OH...OC appear at 3462, 3372, 3264 and 3100 cm^{-1} respectively when demineralization is carried out at 0.8 M HCl. The most prominent bond in this sample is the OH(6)...OC, which is 54.6% of the total amount followed by CO...HN with 38.0%, OH...OC with 5.4% and OH(3)...O (5) with 2 .%. The amount of OH(6)...OC and CO...HN drop to 28.43 and 35.23% while the portion of OH(3)...O(5) and OH...OC rise to 28.50 and 7.84% respectively when shrimp shell is treated

Table 3
Crystalline index and size of shrimp chitin with concentrations of HCl and NaOH.

HCl:NaOH (M)	D_{110} (Å)	D_{130} (Å)	D_{013} (Å)	CrI (%)
0.4:0.4	0.0544	0.0757	0.124	87.4
0.4:0.8	0.0548	0.076	0.126	87.0
0.4:1.2	0.0552	0.0762	0.128	86.3
0.8:0.4	0.0568	0.0805	0.141	86.2
0.8:0.8	0.0602	0.0883	0.176	85.4
0.8:1.2	0.0747	0.1280	1.000	85.2
1.2:0.4	0.0766	0.1340	1.220	83.3
1.2:0.8	0.0768	0.1350	1.340	82.0
1.2:1.2	0.0798	0.1420	3.640	79.4

with 1.2 M HCl and 0.8 M NaOH. The average E_H for this sample is 4.63 kCal. At varying acid concentrations of 0.4, 0.8 and 1.2 M HCl with1.2 M alkali on shrimp shell, Table 2 shows varying bands of the inter and intra molecular bonds with average E_H reducing to 4.99, 4.64 and 4.22 kCal as acid concentration increases. Amount of inter molecular CO...HN bond is ≈33% in each sample while OH...OC varies between 5.65 and 6.08%. In summary, average hydrogen bond reductions have been engendered by gradual removal of *N*-acetyl groups for each sample during acid and alkali treatments (with increasing concentrations) as they prevent the formation of inter and intra molecular hydrogen bonding needed for the formation of hard compacts.

3.3. XRD

The XRD of ground virgin shrimp exoskeleton shown in Fig. 6 reveals the existence of crystalline form of $CaCO_3$ (calcite) and chitin in the organic material. The calcite peaks are located on

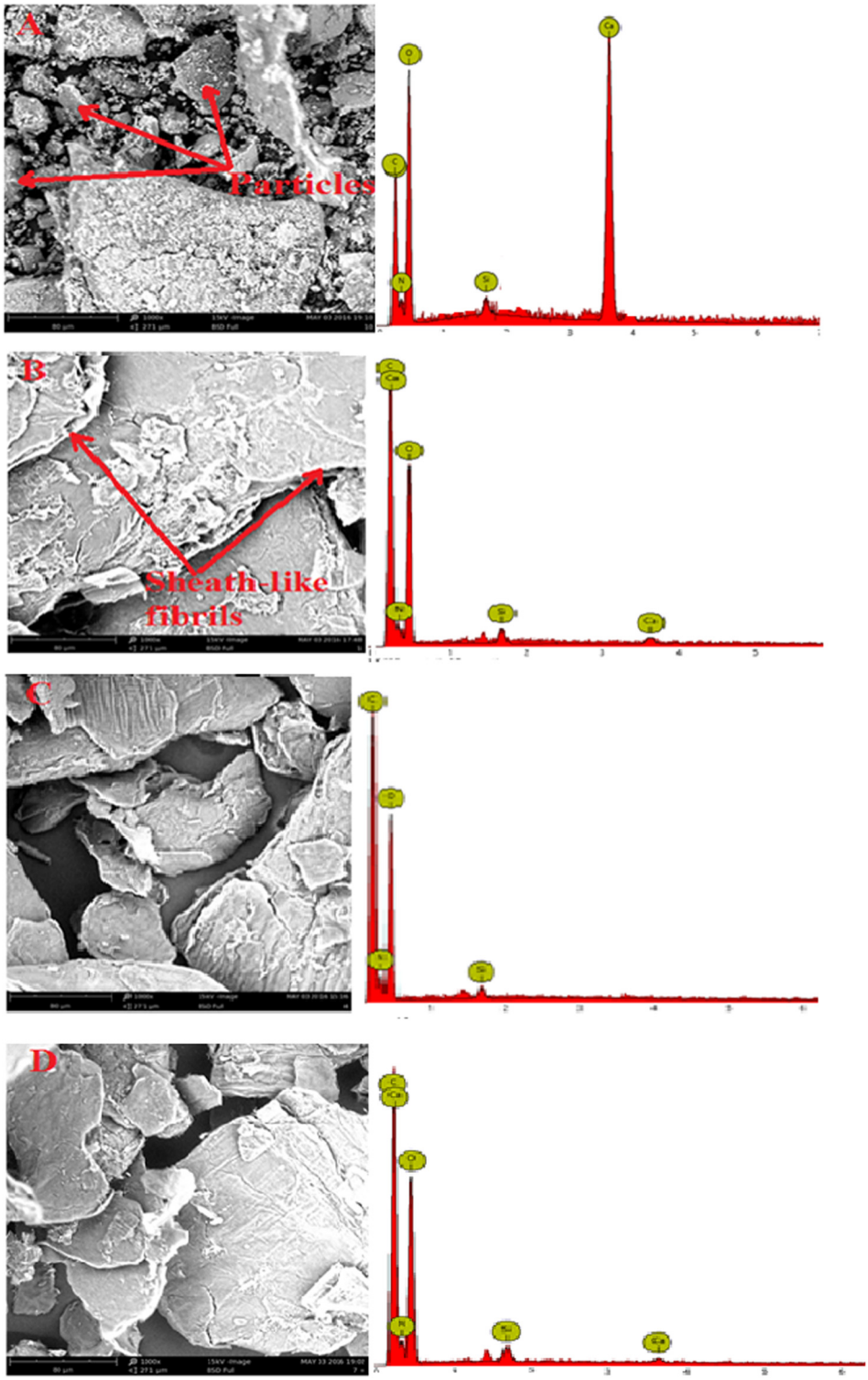

Fig. 10. SEM/EDS images of shrimp shell (a) Virgin (b) treated with 0.4 M HCl (c) 0.8 M HCl (d) 1.2 M HCl at 0.4 M NaOH.

(1 0 4), (1 1 $\bar{3}$) and (1 1 $\bar{6}$) planes with corresponding 2θ values of 28, 40.7 and 48.2 while the rest planes are for chitin [10,24]. Unlike crab and coral exoskeletons that show calcite peak at 2θ = 29° on plane (1 0 4) [7,23], the embedded chitin in the shrimp shell shows the strongest intensity at 2θ = 36° on plane (1 1 0). In addition, the diffractogram reveals other weak chitin peaks that are stronger than the calcite peaks. This phenomenon explains why less acid baths were used during demineralization of shrimp shells when compared to other invertebrates' exoskeleton containing more of calcite [11].

X-ray diffraction spectrum of chitin from shrimp exoskeleton is shown in Figs. 7–9. One strong peak (19.2°) corresponding to (1 1 0) with three weak peaks of 12.6, 23.2 and 26.3° diffracting on planes (0 2 1), (1 3 0) and (0 1 3) are observed. In previous XRD studies conducted on α-chitin from various organisms, two strong peaks at 9 and 19° with weak peaks at 12, 21, 23, and 26° were observed in the spectra [13,29,26,19]. XRD study in this work indicates that α-chitin is extracted. From Fig. 7, it is clear that the intensities of the peaks reduce as acid concentration increases. The Crl of chitin at this alkali concentration (0.4 M) is measured as 87.4, 86.2 and 83.3% for 0.4, 0.8 and 1.2 M HCl respectively. Fig. 8 shows that similar crystalline reflections occur on the same planes but at different intensities when deproteinization is done with 0.8 M NaOH. Demineralizing with 0.4 M HCl produces chitin with Crl of 87.4%. Increasing the acid concentration to 0.8 and 1.2 M further reduces the Crl by 1.8 and 5.7%. However, a significant reduction in peak intensity is observed at 1.2 M HCl with 1.2 M NaOH chitin extract (Fig. 9). This is reflected in the lowest Crl (79.4%), while decrease in acid concentration results in increase in Crl of 85.2 and 86.3% for 0.8 and 0.4 M HCl respectively. The structural stability of the chain decreases due to gradual removal of *N*-acetyl groups which eventually scales down its crystallinity. The gradual reduction of Crl is an implication of distortion in chitin's crystal structure arising as concentrations of reagents permit the cleavage of intra and intermolecular hydrogen bonds. Table 3 shows the crystalline sizes of shrimp chitin extracted with varying acid and alkali concentrations.

3.4. SEM/EDS

Fig. 10 shows the SEM/EDS of shrimp shells treated with concentrations of HCl (0.4–1.2 M) at a fixed concentration of NaOH. The EDS of the virgin shrimp shell shows strong calcium and oxygen peaks (Fig. 10a). This implies that the shrimp shell surface

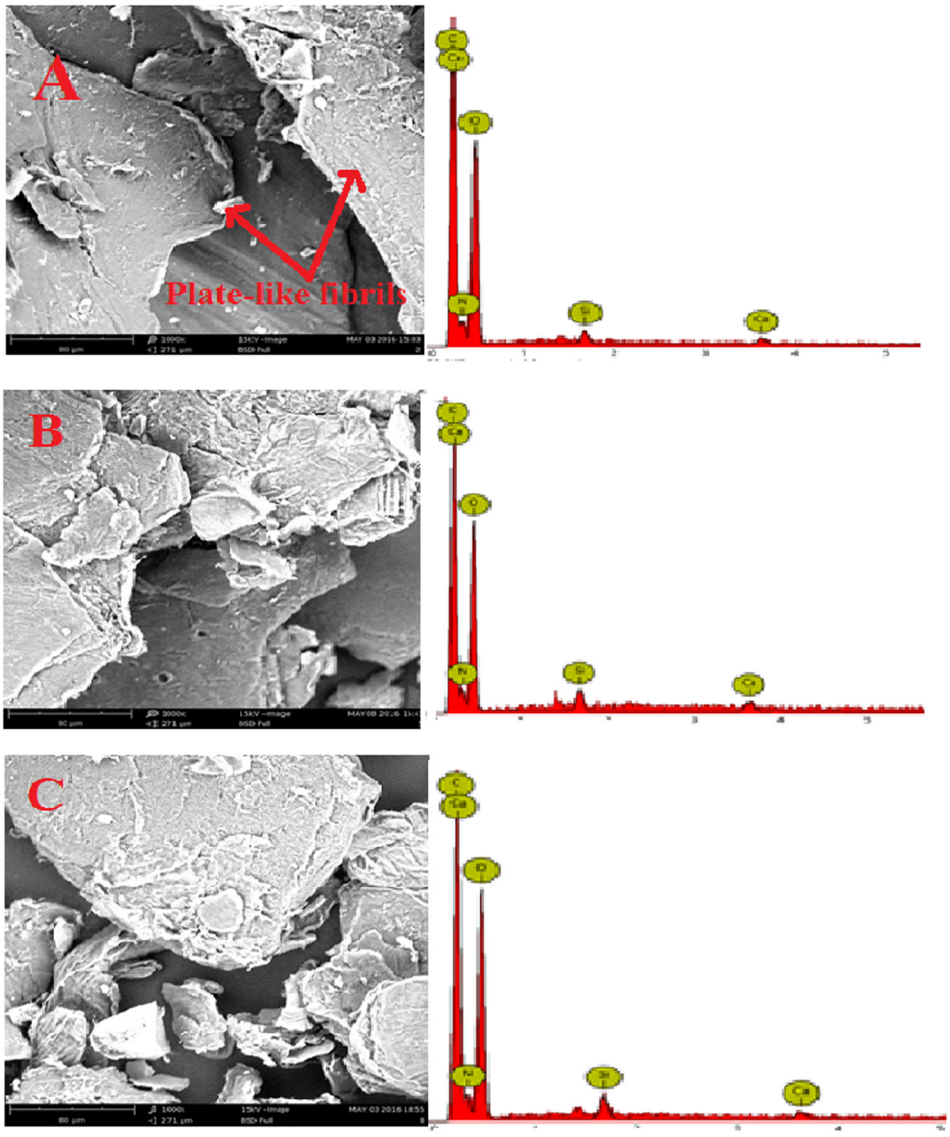

Fig. 11. SEM/EDS images of shrimp shell treated with (a) 0.4 M HCl (b) 0.8 M HCl (c) 1.2 M HCl at 0.8 M NaOH.

consists of calcite and other trace elements such as nitrogen and silicon. Treatment with 0.4 M of HCl leads to a significant change in the composition. After exposure to the acid, calcium peak disappears completely giving rise to increase in the count of the carbon and oxygen peaks (Fig. 10b). The EDS microanalysis shows that there is a 94.6% reduction in the amount of calcium and 4% reduction in oxygen. However, carbon content increases by 76%, indicating the formation of α-chitin polymer. This confirms that the calcite in the shell dissolved rapidly in the presence of acid. There is change from a relatively rough surface of the shrimp fibres to a relatively smooth surface of large sized sheath-like fibrils. Increase in concentration of HCl to 0.8 M leads to a significant change in the surface structure of the shrimp shell (Fig. 10c). Rough surfaces of α-chitin are attributed to low DA. This shows that increase in acid concentration reduces DA. The surface looks smoother than that at 0.4 M HCl with an evidence of a fibrillar structure. However, the carbon content appears unchanged. The microanalysis shows a total disappearance of calcium after this treatment, which is buttressed by the smoothness of the treated shells' surface morphology. A similar change is also observed at 1.2 M HCl treatment (Fig. 10d). The surface smoothness is found to increase with increase in acid concentration. However, further increase in concentration decreases the fibril size but with smoother morphology. Similar images were reported for α-chitin from shrimp and *H. parallela* by Liu et al. [19]. The sheath-like nature of chitin was also noted by Isa et al. [11].

The effect of increase in NaOH concentration to 0.8 M with HCl concentrations on the surface morphology and micro-constituents of the treated shells is shown in Fig. 11. Treatment of this sample with 0.8 M alkali and 0.4 M acid leads to removal of calcite and formation of α-chitin fibril structure as indicated by the SEM/EDS in Fig. 11a. Its microanalysis shows that the treatment leads to 96% removal of calcium, 3.2% removal of oxygen and 74.8% improvement in carbon content. This is a clear indication of the removal of calcium and the formation of carbon-hydrogen chains of the chitin structure. It is also evident that the particle-like substances of the raw shrimp shell morphology (Fig. 10a) are changed to plate-like fibrils with improvement in surface smoothness. Further increase in HCl concentration to 0.8 M produces 4.7% reduction in oxygen content, 92% reduction in calcium and 75% increase in carbon content (Fig. 11b). This result is quite similar to that at 0.4 M acid concentration but with little improvement in oxygen content. The surface morphology also remains the same. Further increase in acid concentration to 1.2 M does not result in a significant difference relative to that at 0.8 M acid (Fig. 11c). However, the fibrils decline in size and are not uniform.

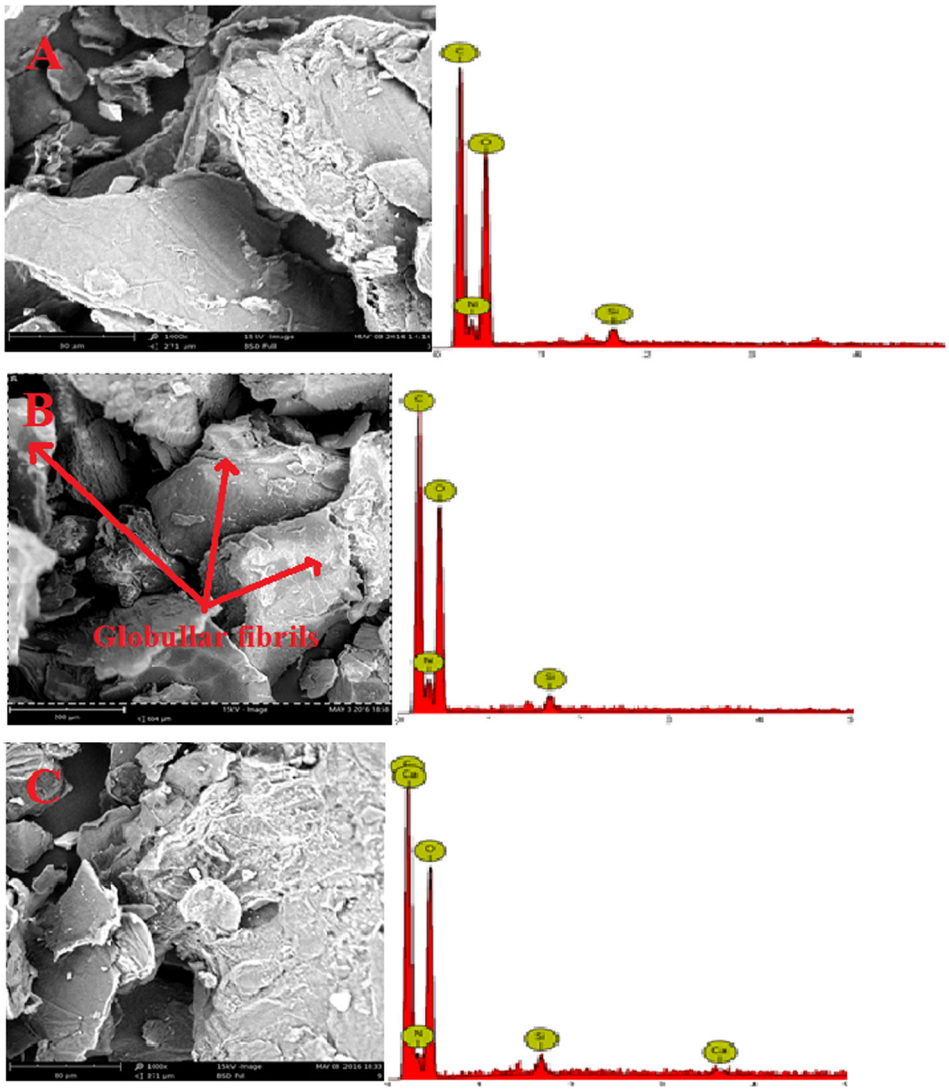

Fig. 12. SEM/EDS images of shrimp shell treated with (a) 0.4 M HCl (b) 0.8 M HCl (c) 1.2 M HCl at 1.2 M NaOH.

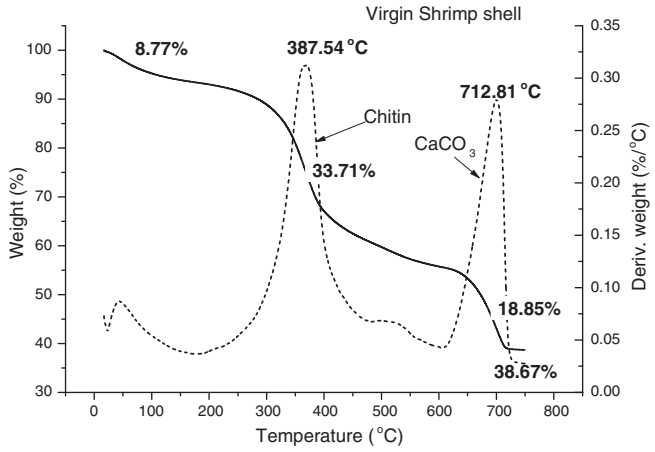

Fig. 13. TGA/DTG curve for virgin shrimp shell.

Fig. 12 shows the effect of further increase in concentration of the alkali to 1.2 M on the surface morphology and micro-constituents of shrimp shells. The microanalysis shows that there is complete removal of calcium from the shrimp shells when treated with 0.4 M of the acid (Fig. 12a). The analysis also records 75% increase in the amount of carbon showing the formation of α-chitin while oxygen is reduced by 4%. This is also shown by the change in particle-like nature of the virgin sample to a more fibrilla structure. The morphology in Fig. 12b shows smooth globules with large surface structures compared to virgin shrimp shell at 0.8 M HCl. Fig. 12c shows the surface morphology of shrimp treated using 1.2 M HCl with the removal of calcite and the formation of fibrillar network of chitin chains.

3.5. TGA

The TGA curve for virgin shrimp shell shows three weight loss steps during thermal decomposition (Fig. 13). The initial weight loss (8.77%) observed between 80 and 110 °C is attributed to the

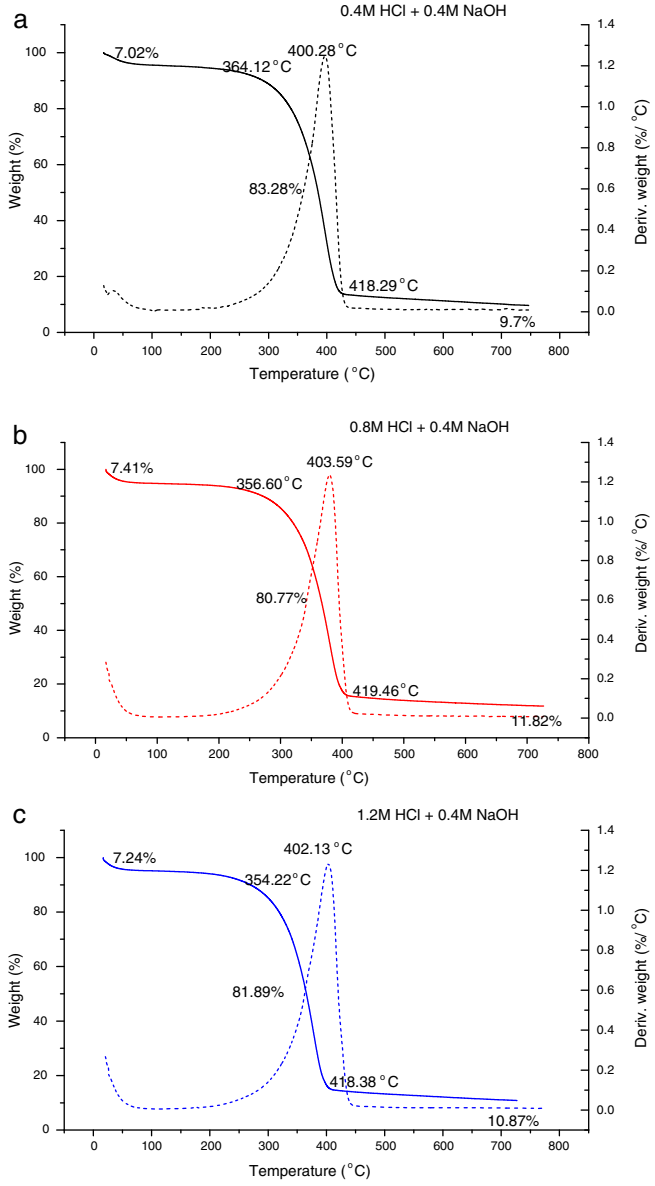

Fig. 14. TGA /DTG curves for chitin extracted from shrimp shell at (a) 0.4 (b) 0.8 (c) 1.2 M HCl and 0.4 M NaOH.

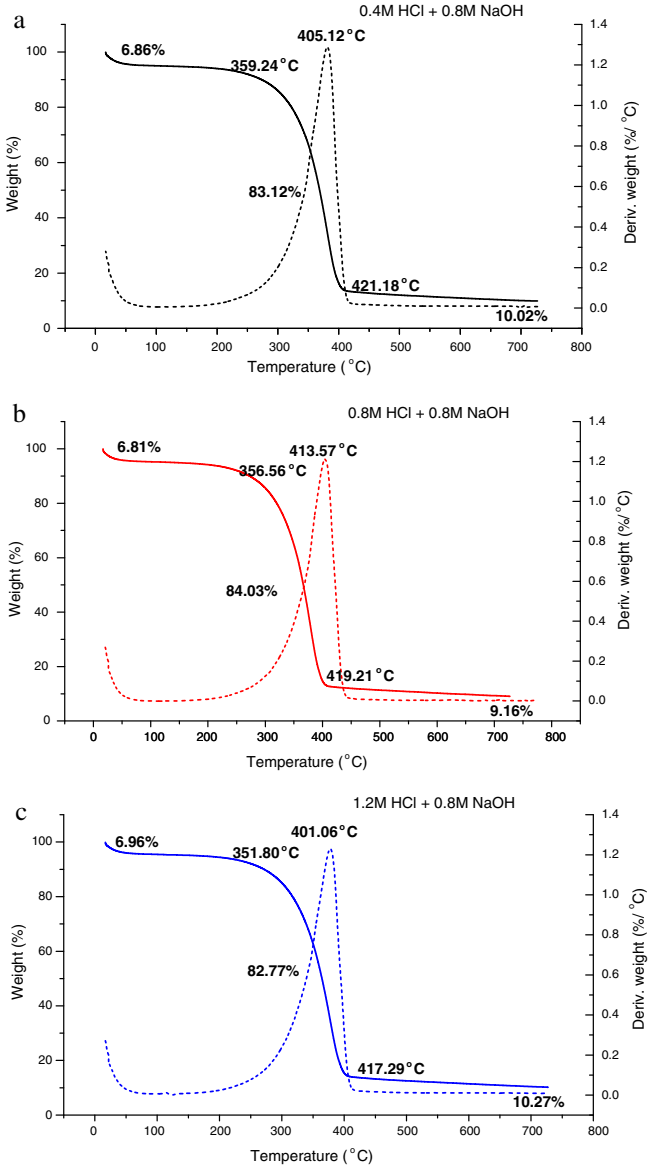

Fig. 15. TGA /DTG curves for chitin extracted from shrimp shell at (a) 0.4 (b) 0.8 (c) 1.2 M HCl and 0.8 M NaOH.

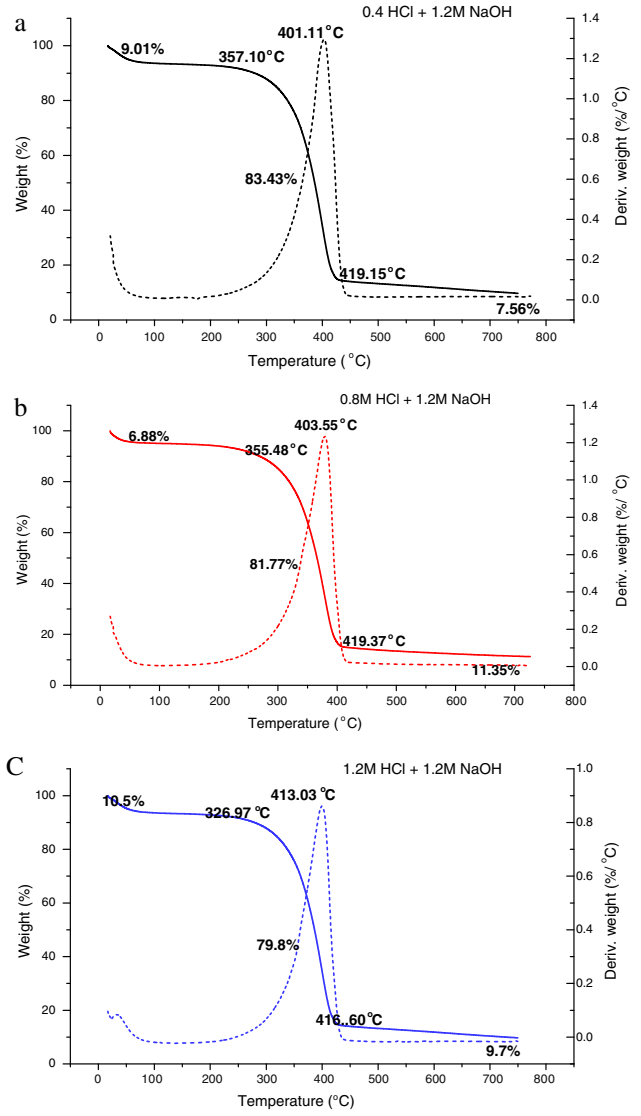

Fig. 16. TGA /DTG curves for chitin extracted from shrimp shell at (a) 0.4 (b) 0.8 (c) 1.2 M HCl and 1.2 M NaOH.

vaporization of water from the sample while degradation of chitin sample starts at higher temperature, precisely after 321.01 °C. Above this temperature, the thermal stability of embedded chitin gradually decreases and its degradation completes at 397.93 °C. This occurs at the second decomposition stage as 33.7% chitin degrades. With temperature in the range 665–713 °C, the 18.85% calcite, $CaCO_3$ contained in shrimp shell is converted to CaO. However, the sample weight is constant until the temperature reaches 750 °C. Improved chitin content (38.2%) was also observed from lobsters in the works of Boßelmann et al. [7], with 16.1% $CaCO_3$ and a residue of 38.67% after decomposition.

Fig. 14 shows the TGA/DTG curves of shrimp shells fully treated using the varying concentrations of acid at 0.4 M NaOH. The degradation of 7.02% starts between 50–100 °C and it is associated with evaporation of water molecules (Fig. 14a). The second stage of decomposition between 364.12–418.29 °C (T_{onset} – T_{finish}) results in the degradation of saccharide structure of the molecules with the dehydration of saccharide rings and decomposition of the acetylated units of chitin. The maximum temperature of degradation T_{max} for chitin at this second step is recorded at 400.28 ° C for 0.4 M treated shell (Fig. 14a) while 403.59 and 402.13 °C are measured for 0.8 and 1.2 M HCl treated samples respectively (Fig. 14b and c). Chitin content of 83.28, 80.77 and 81.89% are observed for samples demineralized at 0.4, 0.8 and 1.2 M HCl respectively The T_{max} disintegration temperatures of α-chitin extracted from krill and coral shells in previous studies ranged between 370 and 372 °C [12,1]. The difference in disintegration temperatures of extracted chitins compared with this present study (400–403 °C) shows that different values can be obtained from different aquatic invertebrates.

As shown in Fig. 15a–c, TGA/DTG thermograms for chitin deproteinized with 0.8 M alkali reveal mainly two decomposition steps where the first stage occurs in the range 40–100 °C and attributed to free water evaporation with a 6–9% weight loss. In the second stage, the T_{onset} of the polysaccharide ranges between 351 and 369 °C while T_{finish} lies within 417 and 421 °C. The highest chitin content of 84.03% is recorded with the use of 0.8 M HCl and 0.8 M NaOH (Fig. 15b) while demineralizing with 0.4 and 1.2 M HCl culminate in 83.12 and 82.77% chitin contents (Fig. 15a and c). Works of Andrade et al. [4] on shrimp exoskeleton showed that 50% chitin decomposed between 400–500 °C.

TGA and corresponding DTG curves of chitin extracted from varying acid concentrations and at 1.2 M NaOH are shown in Fig. 16a–c. For these samples, the first step from 40 to 140 °C is attributed to water evaporation with 6–11% mass loss. Using 0.4 M HCl treatment (Fig. 16a), 83.43% of chitin is obtained and the degradation of its molecular structure occurs in the range 357.10–419.15 °C. The second decomposition stage for 0.8 M HCl (Fig. 16b) treated sample shows chitin occurrence of 81.77% as evidenced by its decomposition which occurs within 355.48 and 419.37 °C. Fig. 16c shows 79.8% chitin decomposition when shrimp shell is treated with 1.2 M HCl and 1.2 M NaOH. Decomposition occurs between 326.97 and 416.60 °C while the residue produced for the samples are 7.56, 11.35 and 9.7% for 0.4, 0.8 and 1.2 M HCl treated samples respectively. Thermal stability of chitin embedded in shrimp shell (Fig. 13) is lower compared to their corresponding isolated forms as its T_{onset} possesses the least value (321 °C). This is also evident with their T_{max} and T_{finish} values. Increasing acid and alkali concentrations leads to the reduction of samples' T_{onset} which implies gradual lowering of thermal stability.

4. Conclusions

In this study, increasing concentrations of acid and alkali gradually reduce the acetyl units in chitin producing considerable proportion of amino units. The resistance of acetamide groups imposed by the *trans* arrangement of the C2-C3 substituent in the pyranose ring gradually reduces during this process. The decline in chitin's DA promotes creation of hydrogen bond cleavage that leads to alterations in chitin's crystal structure as demonstrated by the decrease in CrI. This study has also shown that HCl induces partial removal of the *N*-acetyl groups leading to decrease in DA at increasing concentrations. The EDS of shrimp exoskeleton shows that its surface is made of calcite and other trace elements such as nitrogen and silicon. The surface smoothness increases with increase in acid concentration. TGA result shows that thermal stability of fully extracted chitin is greater than that of chitin embedded in the shrimp exoskeleton. This is achieved when $CaCO_3$, proteins and other pigments are removed from the exoskeleton which increases the magnitude of T_{onse}, T_{finish} and T_{max}. The magnitude of chitin average E_H is majorly influenced by OH(6)...OC intra and CO...HN intermolecular hydrogen bonds as they show more predominance than OH(3)---O(5) and OH...OC intra and intermolecular hydrogen bonds respectively. The results of this study compared to observations from other studies have shown that treatment parameters used and geographical location

of aquatic animals' shells under investigation influence the physicochemical properties of extracted chitin.

Acknowledgements

The authors thankfully acknowledge the University of Lagos-Nigeria, Redeemer's University-Nigeria, Covenant University-Nigeria and Soochow University-China for making their facilities available for this work.

References

[1] E.S. Abdou, K.S.A. Nagy, M.Z. Elsabee, Extraction and characterization of chitin and chitosan from local sources, Bioresour. Technol. 99 (2008) 1359–1367.
[2] F.A. Al Sagheer, M.A. Al-Sughayer, S. Muslim, M.Z. Elsabee, Extraction and characterization of chitin and chitosan from marine sources in Arabian Gulf, Carbohydr. Polym. 77 (2009) 410–419.
[3] R.R. Ambati, S.M. Phang, S. Ravi, R.G. Aswathanarayana, Astaxanthin: sources, extraction, stability, biological activities and its commercial applications—a review, Marine Drugs 12 (2014) 128–152.
[4] S.M.B. Andrade, B. Ladchumananandasivam, B.G. Rocha, D.D. Belarmino, A.O. Galvão, The use of exoskeletons of shrimp (Litopenaeus vanammei) and crab (Ucides cordatus) for the extraction of chitosan and production of nanomembrane, Mater. Sci. Appl. 3 (2012) 495–508.
[5] I. Aranaz, M. Mengíbar, R. Harris, I. Paños, B. Miralles, N. Acosta, G. Galed, A. Heras, Functional characterization of chitin and chitosan, Curr. Chem. Biol. 3 (2009) 203–230.
[6] W. Arbia, L. Arbia, L. Adour, A. Amrane, Chitin extraction from crustacean shells using biological methods—a review, Food Technol. Biotechnol. 51 (2013) 12–25.
[7] F. Boßelmann, P. Romano, H. Fabritius, D. Raabe, M. Epple, The composition of the exoskeleton of two crustacea: The American lobster Homarus americanus and the edible crab Cancer pagurus, Thermochim. Acta 463 (2007) 65–68.
[8] D. Ciolacu, J. Kovac, V. Kokol, The effect of the cellulose-binding domain from clostridium cellulovorans on the supramolecular structure of cellulose fibres, Carbohydr. Res. 345 (2010) 621–630.
[9] J. Cui, Z. Yu, Z.D. Lau, Effect of acetyl group on mechanical properties of chitin/chitosan nanocrystal: A molecular dynamics study, Int. J. Mol. Sci. 17 (2015) 1–13.
[10] J. Felsen, A. Žalga, A. Kareiva, Characterization of naturally derived calcium compounds used in food industry, Chemija 23 (2012) 76–85.
[11] M.A. Isa, A.O. Ameh, J.O. Gabriel, K.K. Adama, Extraction and characterization of chitin from Nigerian sources, Leonardo Electr. J. Pract. Technol. 21 (2012) 75–81.
[12] B.A. Juárez-de la Rosa, J.M. Crespo, Q. Owen, W.S. Gónzalez-Gómez, J.M. Yañez-Limón, J.J. Alvarado-Gil, Thermal analysis and structural characterization of chitinous exoskeleton from two marine invertebrates, Thermochim. Acta 610 (2015) 16–22.
[13] B.A. Juarez-de la Rosa, P. Quintana, P.L. Ardisson, J.M. Ya'nez-Limon, J.J. Alvarado-Gil, Effects of thermal treatments on the structure of two black coral species chitinous exoskeleton, J. Mater. Sci. 47 (2012) 990–998.
[14] M. Kaya, O. Seyyar, T. Baran, T. Turkes, Bat guano as new and attractive chitin and chitosan source, Front. Zool. 11 (2014). 1-1-10.
[15] S. Kim, Chitin, chitosan, oligosaccharides and their derivatives; biological and their applications, Taylor and Francis Group (2011) 3–633.
[16] Kittle, J.D., (2012). Characterization of cellulose and chitin thin films and their interactions with bio-based polymers. Dissertation submitted to Virginia Polytechnic Institute and State University. 1–186.
[17] J. Kumirska, M.X. Weinhold, M.C. Czerwicka, Z. Kaczyński, A. Bychowska, K. Brzozowski, J. Thöming, P. Stepnows, Influence of the Chemical Structure and Physicochemical Properties of Chitin- and Chitosan-Based Materials on their Biomedical Activity, Biomedical Engineering, Trends in Materials Science, 2011, pp. 25–64.
[18] Z. Limam, S. Selmi, S. Sadok, A. El Abed, Extraction and characterization of chitin and chitosan from crustacean by-products. Biological and physicochemical properties, Afr. J. Biotechnol. 10 (2011) 640–647.
[19] S. Liu, J. Yu, C. Bi, F.Q.u.M. Zhu, C Jiang, Q. Yang, Extraction and characterization of chitin from the beetle holotrichia parallela motschulsky, Molecules 17 (2012) 4604–4611.
[20] F.G. Malinovsky, J.U Fange, W.I.G. Willats, The role of the cell wall in plant immunity, Front. Plant Sci. 5 (2014) 1–12.
[21] Y.S. Nam, W.H. Park, D. Ihm, S.M. Hudson, Effect of the degree of deacetylation on the thermal decomposition of chitin and chitosan nanofibers, Carbohydr. Polym. 80 (2010) 291–295.
[22] B. Park, M.M. Kim, Applications of chitin and its derivatives in Biological medicine, Int. J. Mol. Sci. 11 (2010) 5152–5164.
[23] M.A. Rahman, J. Halfar, First evidence of chitin in calcified coralline algae: new insights into the calcification process of clathromorphum compactum, Sci. Rep. (2014) 1–11.
[24] I. Raya, E. Mayasari, A. Yahya, M. Syahrul, A. Latunra, Shynthesis and characterizations of calcium hydroxyapatite derived from crabs shells (Portunus pelagicus) and its potency in safeguard against to dental demineralizations, Int. J. Biomater. (2015) 1–9.
[25] J. Rojas, C. Hernandez, D. Trujillo, Effect of the alkaline treatment conditions on the tableting performance of chitin obtained from shrimp heads, Afr. J. Pharm. Pharmacol. 8 (2014) 211–219.
[26] W. Sajomsang, P. Gonil, Preparation and characterization of α-chitin from cicada sloughs, Mater. Sci. Eng., C 30 (2010) 357–363.
[27] R.G. Sharp, A review of the applications of chitin and its derivatives in agriculture to modify plant-microbial interactions and improve crop yield, Agronomy 3 (2013) 757–793.
[28] Y. Wang, Y. Chang, L. Yu, C. Zhang, X. Xu, Y. Xue, Z. Li, C. Xue, Crystalline structure and thermal property characterization of chitin from Antarctic krill (Euphausia superba), Carbohydr. Polym. 92 (2013) 90–97.
[29] M.T. Yen, J.H. Yang, J.L. Mau, Physicochemical characterization of chitin and chitosan from crab shells, Carbohydr. Polym. 75 (2009) 15–21.
[30] I. Younes, M. Rinaudo, Chitin and chitosan preparation from marine sources. structure, properties and applications, Marine Drugs 13 (2015) 1133–1174.
[31] Y. Zhao, W.T. Ju, G.H. Jo, W.J. Jung, R.D. Park, Perspectives of chitin deacetylase research, Biothechnol. Polym. (2011) 131–144.
[32] F. Guo, K. Kikuchi, Y. Matahira, K. Sakai, K. Ogawa, Water-soluble chitin of low degree of deacetylation, J. Carbohydr. Chem. 21 (2002) 149–161.
[33] Y. Liu, Z. Liu, W. Pan, Q. Wu, Absorption behaviors and structure changes of chitin in alkali solution, Carbohydr. Polym. 72 (2008) 235–239.